

The Abrupt Shift of Typhoon Activity in the Vicinity of Taiwan and Its Association with Western North Pacific–East Asian Climate Change

JIEN-YI TU

Department of Atmospheric Sciences, Chinese Culture University, Taipei, Taiwan

CHIA CHOU

Research Center for Environmental Changes, Academia Sinica, and Department of Atmospheric Sciences, National Taiwan University, Taipei, Taiwan

PAO-SHIN CHU

Department of Meteorology, SOEST, University of Hawaii at Manoa, Honolulu, Hawaii

(Manuscript received 4 January 2008, in final form 14 January 2009)

ABSTRACT

Bayesian analysis is applied to detect changepoints in the time series of seasonal typhoon counts in the vicinity of Taiwan. An abrupt shift in the typhoon count series occurs in 2000. On average, 3.3 typhoons per year have been noted before 2000 (1970–99), with the rate increasing to 5.7 typhoons per year since 2000 (2000–06). This abrupt change is consistent with a northward shift of the typhoon track over the western North Pacific–East Asian region and an increase of typhoon frequency over the Taiwan–East China Sea region. The northward shift of the typhoon track tends to be associated with typhoon-enhancing environmental conditions over the western North Pacific, namely, the weakening of the western North Pacific subtropical high, the strengthening of the Asian summer monsoon trough, and the enhanced positive vorticity anomalies in the lower troposphere. Based on observational analysis and model simulations, warm sea surface temperature anomalies over the equatorial western and central Pacific appear to be a major factor contributing to a northward-shifted typhoon track.

1. Introduction

Typhoons are one of the most extreme natural events over the western North Pacific–East Asian (WNP–EA sector). Typhoons often affect the spatial distribution of regional precipitation in summer since they are a major source of rainfall over this region. For example, in 2004, 10 typhoons occurred in Japan and brought more than usual precipitation, causing widespread damage, whereas drought occurred in the Philippines and southern China (Kim et al. 2005; Levinson et al. 2005; Wu et al. 2005). Typhoon-related climate studies often focus on the variation of typhoon intensity, frequency, and track in multitemporal scales ranging from intraseasonal to inter-

decadal (Chan 1985, 2000; Chia and Ropelewski 2002; Chu 2004; Ho et al. 2006; Matsuura et al. 2003; Wang and Chan 2002). In recent years, the influence of global warming on the intensity of tropical cyclones has received much attention. Emanuel (2005), Hoyos et al. (2006), and Webster et al. (2005) found increasing trends in the western Pacific and Atlantic based on some available best-track datasets. Chan and Liu (2004) and Klotzbach (2006) found small or no trends using alternate analysis techniques. Other studies (e.g., Landsea et al. 2006) have shown opposite trends to those found by Emanuel in the west Pacific by examining other best-track datasets.

In addition to the increase in tropical cyclone intensity, one study also found a detectable shift of the typhoon track over the WNP–EA in the past four decades (Wu et al. 2005). Such a change also affects regional precipitation (Ren et al. 2006). For a future climate projection, the typhoon track over the WNP–EA region may potentially be affected by global warming (Wu and

Corresponding author address: Chia Chou, P.O. Box 1-48, Research Center for Environmental Changes, Academia Sinica, Taipei 11529, Taiwan.
E-mail: chiachou@rcec.sinica.edu.tw

Wang 2004). In our study, we also focus on the variation of typhoon tracks, particularly on the abrupt change of typhoon tracks from a historical perspective. Observational data for Taiwan are useful for studying variations of typhoon tracks over the WNP–EA region because of the island’s unique location. Taiwan is located at the turning point of the track for most typhoons in the WNP–EA region (Camargo et al. 2007). Figure 1 shows two major typhoon paths over the WNP–EA region: one is moving westward to the South China Sea directly and the other is turning north to either Japan or Korea. Taiwan is located just between these two major tracks, so the number of typhoon landfalls on Taiwan is sensitive to the shift of the typhoon track. Thus, we use the number of typhoons that passed through the vicinity of Taiwan (21° – 26° N, 119° – 125° E) as an index to examine the variation of the typhoon track in the WNP–EA region. The data and statistical methods used in this study are discussed in section 2. We first identified the abrupt shift of the typhoon track in section 3 and then discussed its association with large-scale environmental changes in section 4, followed by a discussion and conclusions.

2. Data, statistical methods, and climate model

a. Data

The number of typhoons in the vicinity of Taiwan from 1970 to 2006 is provided by the Central Weather Bureau (CWB) in Taiwan (Chu et al. 2007). Independently, the typhoon-track information is obtained from the Regional Specialized Meteorological Center (RSMC) Tokyo—Typhoon Center. Here we defined the maximum surface wind over 34 kt as a typhoon case. To understand the influence of the large-scale environment on typhoon activity, the following two global datasets were analyzed: 1) a monthly optimum interpolation (OI) sea surface temperature (SST) with 1° spatial resolution from January 1982 to July 2007 (Reynolds et al. 2002), and 2) other large-scale variables, such as the geopotential height and wind field, are derived from (1979–2006) the National Centers for Environmental Prediction/Department of Energy (NCEP/DOE) Reanalysis 2 (NCEP-2) data (Kanamitsu et al. 2002), with a horizontal resolution of 2.5° latitude \times 2.5° longitude. To be consistent with the SST data, only 25 yr (1982–2006) of the NCEP-2 data are used for composites in this study.

b. Methods

1) BAYESIAN APPROACH FOR DETECTION OF SHIFT IN TYPHOON COUNT SERIES

To detect abrupt shifts in tropical cyclone records, we use a Bayesian changepoint analysis (Chu and Zhao

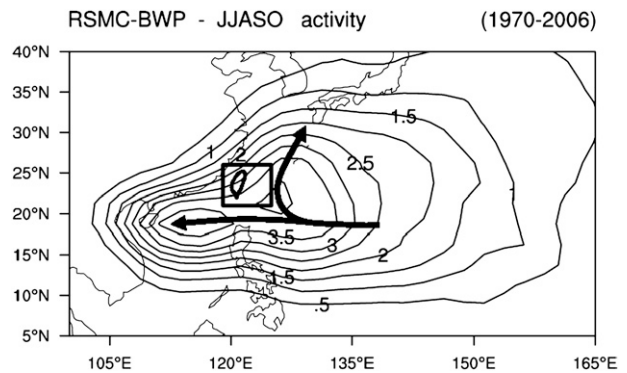


FIG. 1. JJASO typhoon frequency climatology averaged over the period of 1970–2006. The contour interval (CI) is 0.5 per season (JJASO) per grid box ($2.5^{\circ} \times 2.5^{\circ}$). The bold arrows represent the majority of typhoon paths in the western North Pacific–East Asian region. The box represents the area in the vicinity of Taiwan.

2004; Zhao and Chu 2006). Because typhoon occurrence in the study domain is regarded as a rare event, a Poisson process is applied to provide a reasonable representation of typhoon frequency. Poisson process is governed by a single parameter: the Poisson intensity. Given the Poisson intensity, also known as the rate parameter λ , the probability mass function (PMF) of h counts occurring in T unit seasons is (Epstein 1985)

$$P(h|\lambda, T) = \exp(-\lambda T) \frac{(\lambda T)^h}{h!}, \quad \text{where} \\ h = 0, 1, 2, \dots \quad \text{and} \quad \lambda > 0, T > 0. \quad (1)$$

The Poisson mean is the product of λ and T , and so is its variance.

In many real applications adopting the model (1), the rate parameter λ is treated as a random variable instead of a constant to construct a hierarchical framework (e.g., Chu and Zhao 2004; Elsner and Jagger 2004). A functional choice of the prior for λ is its conjugate gamma distribution (Epstein 1985) that is formulated by

$$P(\lambda|h', T') = \frac{T'^{h'} \lambda^{h'-1}}{\Gamma(h')} \exp(-\lambda T'), \\ \lambda > 0, h' > 0, \quad \text{and} \quad T' > 0, \quad (2)$$

where the gamma function is defined by $\Gamma(x) = \int_0^{\infty} t^{x-1} e^{-t} dt$. That is, given h counts occurring in T years, if the prior density for λ is gamma distributed with parameters h' and T' , the resulted posterior density for λ is also gamma distributed with parameters $h + h'$ and $T + T'$.

Under the statistical model introduced above, the marginal PMF of h counts occurring in T years is a negative binomial distribution (Epstein 1985) when the

intensity is gamma distributed with prior parameters h' and T' :

$$\begin{aligned}
 P(h|h', T', T) &= \int_0^\infty P(h|\lambda, T)P(\lambda|h', T')d\lambda \\
 &= \frac{\Gamma(h+h')}{\Gamma(h')h!} \left(\frac{T'}{T+T'}\right)^{h'} \left(\frac{T}{T+T'}\right)^h \\
 &= P_{nb}\left(h|h', \frac{T'}{T+T'}\right), \tag{3}
 \end{aligned}$$

where $h = 0, 1, \dots$, $h' > 0$, $T' > 0$, $T > 0$, and $P_{nb}(\cdot)$ stands for negative binomial distribution. The prior parameters h' and T' can be estimated using the moment method (Carlin and Louis 2000; Chu and Zhao 2004).

As gleaned from (1) and (2), seasonal typhoon counts near Taiwan are described by a Poisson model whose rate is conditional on a gamma distribution. We consider a hypothesis space for the seasonal typhoon rate. That is, there is either no change in the rate or a single change in the rate (Chu and Zhao 2004). For the first hypothesis (H_0), the distribution for Poisson intensity is assumed as being time invariant. If the two prior parameters h' and T' are given, it is fairly straightforward to generate the conditional posterior density function for λ . For the second hypothesis (H_1), since a single changepoint is assumed, distribution for the seasonal rate before the changepoint is different from that after the changepoint. Thus, two different Poisson models are invoked, and each rate is then conditional on its own gamma density. As a result, four prior parameters need to be given to generate the conditional posterior densities for two Poisson intensities and the conditional posterior density of the changepoint. Because we do not have any credible prior information for the potential changepoint, we opt to use a uniform distribution. For the hypothesis models, a noninformative prior is used. That is, $P(H_0) = P(H_1) = 1/2$. This is justified by the fact that there is no prior information regarding which one of the hypotheses is preferable.

2) CLASSICAL CHANGEPOINT ANALYSIS

In addition to tropical cyclones, it is also of interest to investigate whether there is any changepoint in the SST records or typhoon passage frequency series. Because these variables do not follow a Poisson process, we use a different method to detect abrupt shifts in the temperature or passage frequency series: a log-linear regression model in which a step function is expressed as an independent variable is adopted. If the estimated slope is at least twice as large as its standard error, one would reject the null hypothesis (i.e., with the slope being zero) at the 5% significance level. This model is similar to that used in Elsner et al. (2000) and Chu (2002).

3) A NONPARAMETRIC TEST FOR THE DIFFERENCES IN LOCATION

To evaluate the difference in the mean circulation between two samples, we use a classic nonparametric test, known as the Wilcoxon–Mann–Whitney test (Chu 2002). To perform this test, the two data batches need to be pooled together and ranked. The null hypothesis assumes that the two batches come from the same distribution.

Assume that we have two batches of sample data, with sample sizes n_1 and n_2 ($n = n_1 + n_2$), respectively. To perform this test, the two data batches need to be pooled and ranked. Let U be the Mann–Whitney statistic

$$\begin{aligned}
 U_1 &= R_1 - \frac{n_1}{2}(n_1 + 1) \\
 U_2 &= R_2 - \frac{n_2}{2}(n_2 + 1), \tag{4}
 \end{aligned}$$

where R_1 and R_2 are defined as the sum of the ranks held by batches 1 and 2, respectively. The null distribution of the Mann–Whitney U statistic is approximately Gaussian when n_1 or n_2 is moderately large, with

$$\mu_U = \frac{n_1 n_2}{2}, \tag{5}$$

$$\sigma_U = \left[\frac{n_1 n_2 (n_1 + n_2 + 1)}{12} \right]^{1/2}. \tag{6}$$

Once μ_U , σ_U , and U_1 (or U_2) are computed, the U statistic at each grid point is transformed into a standard Gaussian variable and is evaluated for its statistical significance.

c. Model

A coupled ocean–atmosphere–land model of intermediate complexity (Neelin and Zeng 2000; Zeng et al. 2000) is used in this study. Based on the analytical solutions derived from the Betts–Miller moist convective adjustment scheme (Betts and Miller 1993), typical vertical structures of temperature, moisture, and winds for deep convection are used as leading basis functions for a Galerkin expansion (Neelin and Yu 1994; Yu and Neelin 1994). The resulting primitive-equation model makes use of constraints on the flow by quasi-equilibrium thermodynamic closures and is referred to as the quasi-equilibrium tropical circulation model with a single vertical structure of temperature and moisture for deep convection (QTCM1). Because the basis functions are based on vertical structures associated with convective regions, these regions are expected to be well represented

and similar to a general circulation model (GCM) with the Betts–Miller moist convective adjustment scheme.

Instead of coupling a complicated ocean general circulation model, a slab mixed layer ocean model with a fixed mixed layer depth of 50 m is used. By specifying Q flux, which crudely simulates divergence of ocean transport (Hansen et al. 1988, 1997), SST can be determined by the energy balance between surface radiative flux, latent heat flux, sensible heat flux, and Q flux. The Q flux can be obtained from observations or ocean model results (Doney et al. 1998; Keith 1995; Miller et al. 1983; Russell et al. 1985). In general, the Q flux varies from ocean to ocean as well as from season to season. QTCM version 2.3 is used here, with the solar radiation scheme slightly modified.

3. Abrupt shift of typhoon track

A small area of 21°–26°N, 119°–125°E is defined as the vicinity of Taiwan (Chu et al. 2007). If a typhoon passes through this area, we count it as one that influences Taiwan. Figure 2 shows that a majority (over 90%) of typhoons pass through this region in June–October (JJASO), which is a typical typhoon season over the WNP–EA region (Chu et al. 2007). Thus, we count the number of typhoons only for these months of each year, instead of for the entire 12 months. Figure 3a is the time series of seasonal (JJASO) typhoon numbers in the vicinity of Taiwan from 1970 to 2006. The interannual variation is relatively small before 1982, but becomes much stronger after 1982. An increase of the number of typhoons in recent years is also evident. Figure 3b displays the posterior probability mass function of the changepoint plotted as a function of time (year). High probability on year i implies a more likely change occurring, with year i being the first year of a new epoch, or the so-called changepoint. In Fig. 3b, we note a great likelihood of a changepoint on the typhoon rate in 2000. The average typhoon rate is 3.3 yr^{-1} during the first epoch (1970–99), but increased to 5.7 yr^{-1} during the second epoch (2000–06), thus almost doubling from the first to the second. Because there are two parameters to estimate for each epoch, given a changepoint, the minimum sample size is two. To achieve robust results, however, Chu and Zhao (2004) and Zhao and Chu (2006) suggested the use of 5 yr at each end of the dataset to estimate the prior parameters. Because the data observed after the changepoint year in 2000 are quite consistent, showing higher typhoon counts relative to the first epoch, we feel that our approach and the sample size ($n = 7$) are appropriate to establish a consistent estimation for the “after changepoint” period. Separately, a nonparametric test also shows that the

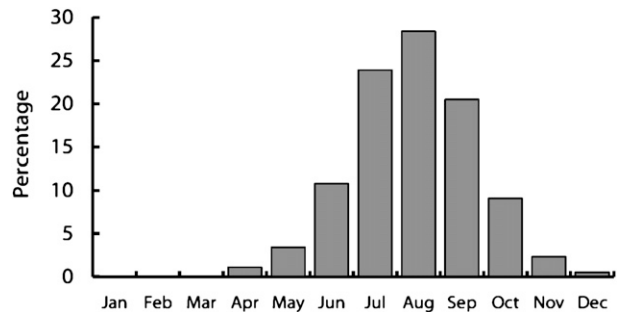


FIG. 2. Monthly percentage of typhoons impacting Taiwan averaged over the period of 1970–2006.

difference of the mean of typhoon numbers (Fig. 3a) between the two epochs is significant at the 5% level. Extending the data further to the typhoon season of 2007, five typhoons were observed in the vicinity of Taiwan, so 2007 is also consistent with the second epoch, with higher typhoon numbers. To further substantiate the abrupt shift in typhoon activity, Fig. 3c displays the posterior density function of the rate parameter before and after the changepoint year. The posterior distribution represents a combination of the prior distribution and the likelihood function. Note the very little overlapping areas in the tail areas between two posterior distributions in Fig. 3c, supporting the notion of a rate increase from the first epoch to the second.

To understand the association of the variation of typhoon number over the vicinity of Taiwan with the spatial distribution of typhoon activity over a larger area, such as the entire WNP–EA region, the frequency of the typhoon occurrence is counted for each 6-h interval for each grid box of $2.5^\circ \times 2.5^\circ$ (Stowasser et al. 2007; Wu and Wang 2004). Figure 3d shows the difference in the mean typhoon rate between the two epochs, that is, the period of 2000–06 minus the period of 1970–99. The spatial distribution exhibits a pronounced increase of typhoon frequency north of 20°N and a decrease south of 20°N over the western part of the WNP–EA region ($100^\circ\text{--}140^\circ\text{E}$), implying a northward shift of the typhoon frequency since 2000. The area with a significance level at the 5% in Fig. 3d (northeast of the Taiwan vicinity) is slightly different from the vicinity of Taiwan defined in Fig. 3a. This is because of the way typhoon counts constructed in Fig. 3a are somewhat different from the typhoon frequency in Fig. 3d, which contains mixed information of typhoon numbers and typhoon translation speed. Examining the total number of typhoon formations over the entire WNP, no noticeable changes are found. However, on a regional scale, we did find a reduction of the formation number over the South China Sea and the Philippine Sea, but

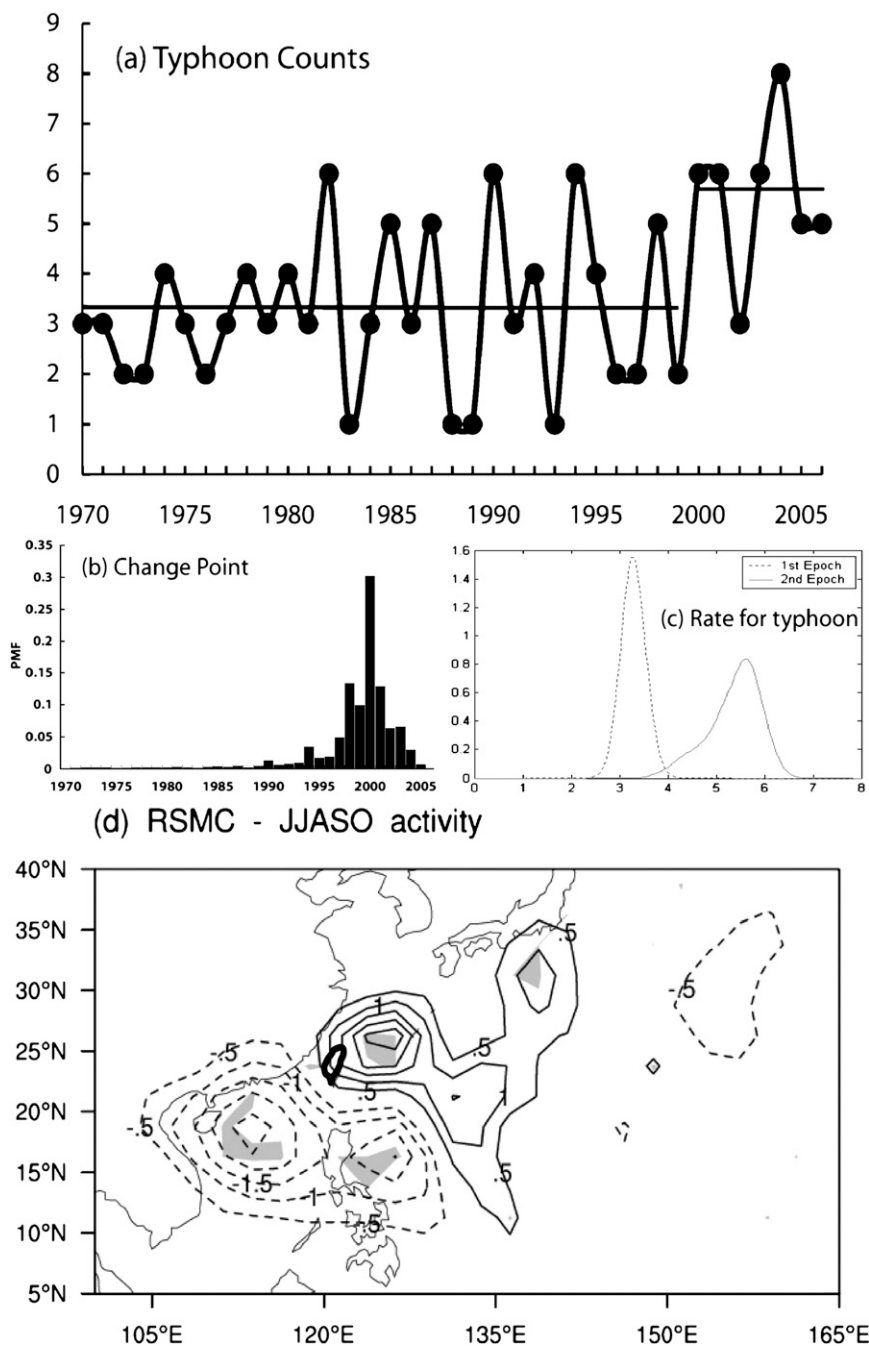


FIG. 3. (a) Time series of seasonal (JJASO) typhoon numbers passing the vicinity of Taiwan from 1970 to 2006 as compiled by the Central Weather Bureau. The vicinity was defined as 21°–26°N, 119°–125°E. (b) The conditional posterior probability mass function of changepoints is plotted as a function of time. (c) Posterior density function of seasonal typhoon rate before (dashed line) and after (solid) the shift, with the changepoint year being set in 2000. (d) June–October typhoon frequency differences for the period of 2000–06 minus the period of 1970–99 from the Regional Specialized Meteorological Center, Tokyo. The CI is 0.5; shading denotes that the difference between the mean of the two epochs is statistically significant at the 5% level.

little change over the vicinity of Taiwan (not shown). Overall, this suggests that the typhoon track over the western part of the WNP–EA region has shifted northward from the South China Sea and the Philippine Sea toward the vicinity of Taiwan and the East China Sea since 2000. Thus, the increased typhoon number over the vicinity of Taiwan after 2000 (Fig. 3a) is not an isolated local feature, but is consistent with the northward shift of the typhoon track over the WNP–EA region.

We further examined the variation of the typhoon frequency in three subregions of the WNP–EA region with large changes of typhoon frequency (Fig. 4): the South China Sea (15° – 20° N, 110° – 120° E), the Philippine Sea (15° – 20° N, 120° – 130° E), and the Taiwan–East China Sea region (25° – 30° N, 120° – 130° E). Over the South China Sea (Fig. 4a), a clear interannual variation and a downward linear trend of typhoon frequency, which is obtained from a simple best-fit (least squares) method, are found during the past 37 yr (1970–2006). The linear trend is consistent with the findings of Wu et al. (2005). This downward trend is related to a reduction in the number of typhoon formations over the South China Sea. Over the Philippine Sea (Fig. 4b), the variation is more likely characterized by a decadal variation with a phase shift around 1975, 1985, and the late 1990s. Over the Taiwan–East China Sea region (Fig. 4c), it shows a similar variation of typhoon frequency to that in Fig. 3a, with a statistically significant shift occurring in 2000 at the 5% level, as confirmed by the classical changepoint analysis described in section 2b. In other words, the abrupt shift of the typhoon frequency in the vicinity of Taiwan is a part of the change over the Taiwan–East China Sea region (Figs. 3a and 4c), not associated with the changes in the South China Sea and the Philippine Sea.

4. The association with the large-scale pattern

To understand possible causes for such a northward shift of the typhoon track, we examine variations of the large-scale environment, such as the westward extension of the Pacific subtropical high ridge between two epochs. Because the SST data start in 1982, the period of 1982–99 is used to represent the first epoch, instead of 1979–99, for consistency in analyzing the spatial distribution of large-scale variables. We note that the difference of the analyzed periods between the typhoon data (e.g., Figs. 3 and 4) and the large-scale variables (Figs. 5 and 6) may cause an inconsistency. Moreover, the small sample size of the second epoch may also create some uncertainties in the composite analysis. However, the composite analysis may yield insight to

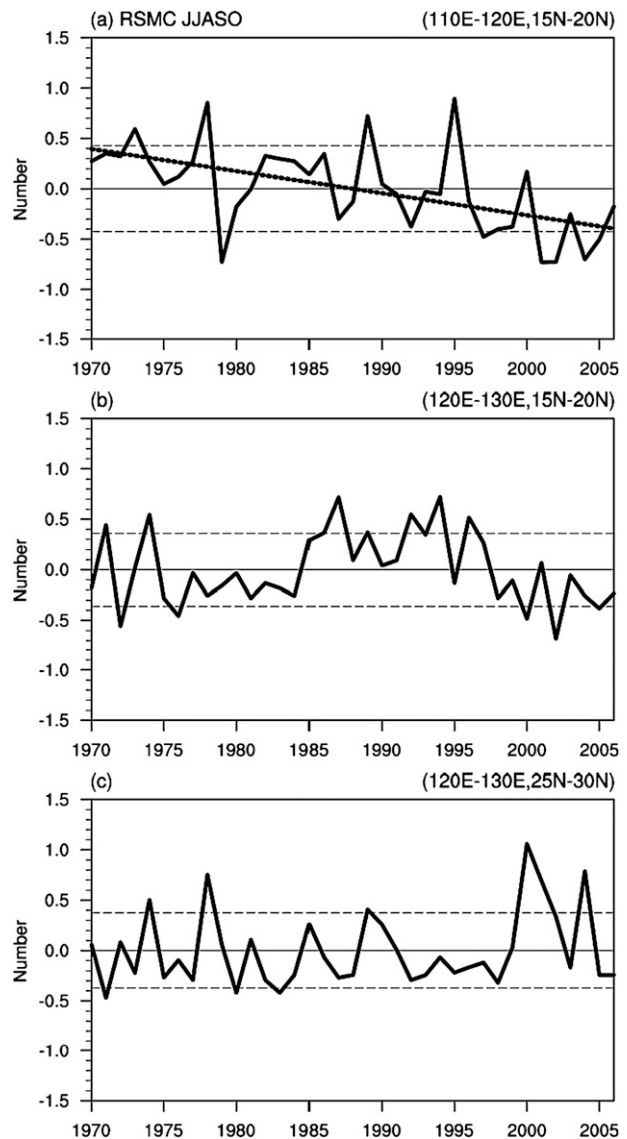


FIG. 4. Time series of seasonal (JJASO) typhoon frequency departure from 1970 to 2006 for three subregions of the western North Pacific: (a) the South China Sea, (b) the Philippine Sea, and (c) the Taiwan and East China Sea region. (top) A best-fit least squares linear trend (thicker dashed line) and one std dev for each area (thinner dashed line). The unit in the y axis is the typhoon number per season (JJASO) per grid box ($2.5^{\circ} \times 2.5^{\circ}$).

the possible mechanisms that induce the abrupt shift of the typhoon number in the Taiwan vicinity.

The ridge of the Pacific subtropical high in the WNP–EA region is the main steering flow controlling the typhoon track (Ho et al. 2004; Wu et al. 2005). Figure 5 shows the 500-hPa geopotential height in the first (dotted line) and second epochs (solid line). The 5880-gpm contour is commonly used to represent the variation of the subtropical high ridge over the WNP–EA region

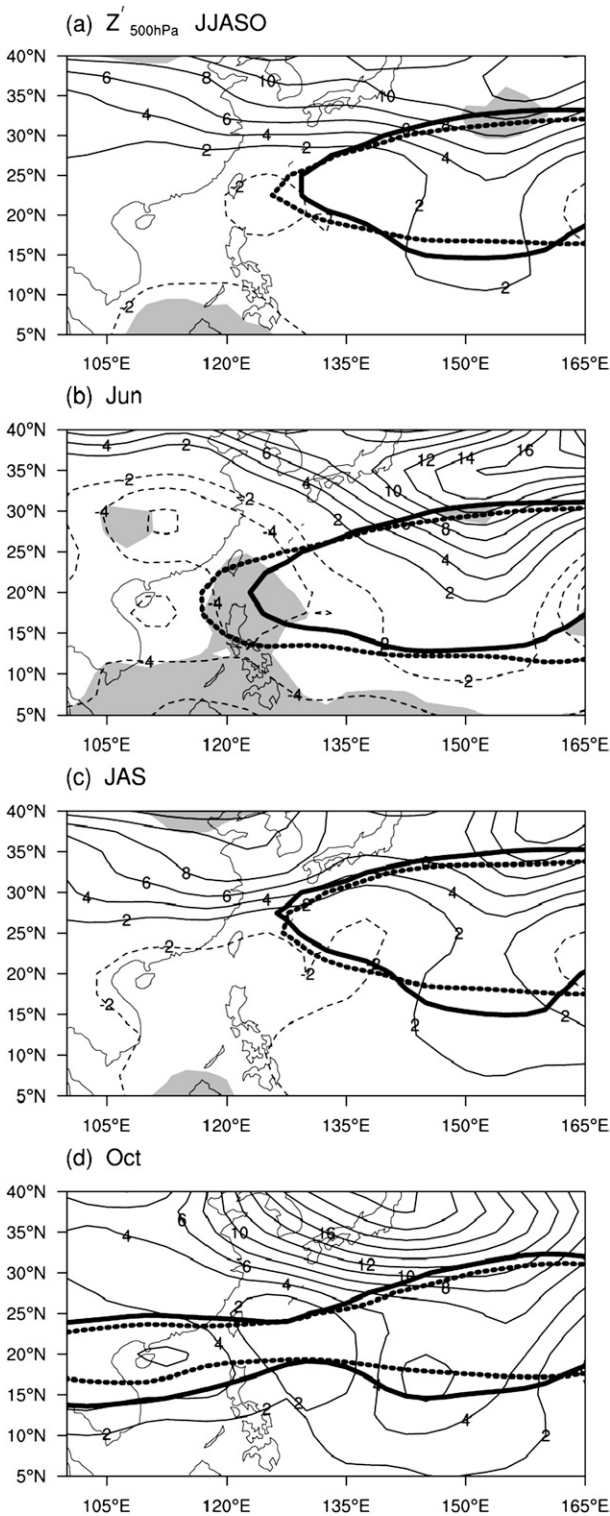


FIG. 5. The 5875-gpm contour of 500-hPa geopotential height for the period of 1982–99 (thick dotted line) and 2000–06 (thick solid line) in (a) JJASO, (b) June, (c) JAS, and (d) October. The contours are the 500-hPa geopotential height differences of the second minus first epoch, shaded by the 10% significance level.

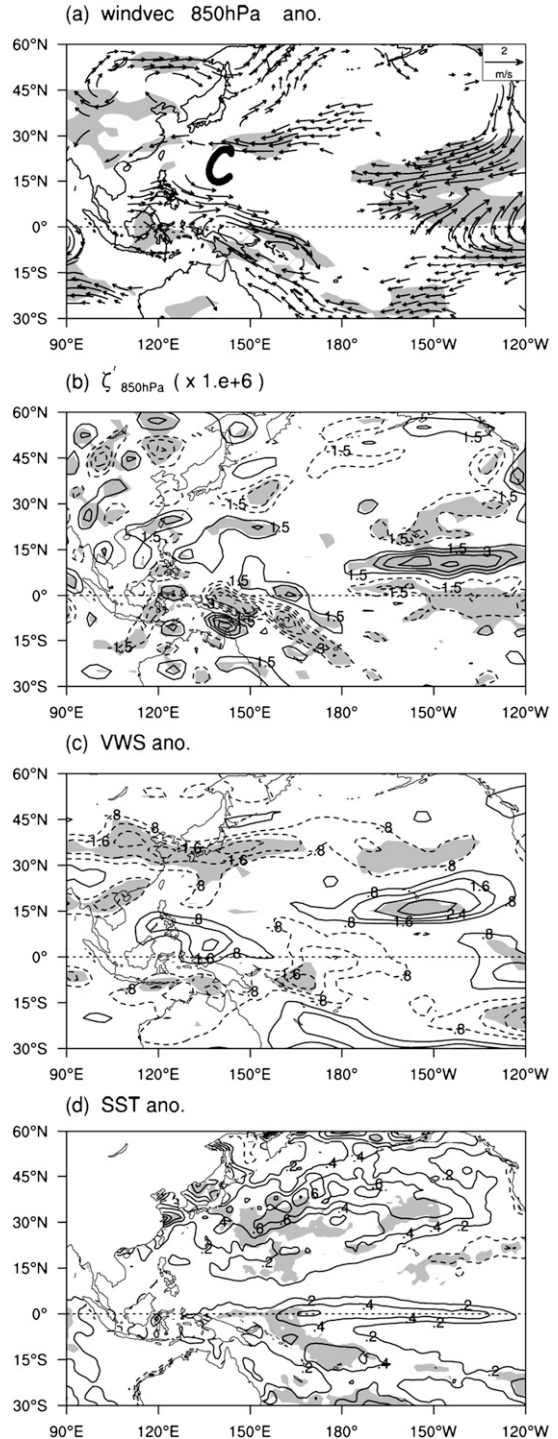


FIG. 6. 850-hPa (a) wind difference and (b) relative vorticity, (c) vertical wind shear (200–850 hPa), and (d) SST between 2000–06 and 1982–99 for JJASO. The CI for 850-hPa relative vorticity is $1.5 \times 10^6 \text{ s}^{-1}$, for vertical wind shear is 0.8 m s^{-1} , and for SST anomalies is 0.2°C . Shading indicates regions where the difference in the mean between two epochs is significant at the 5% level. In (b), (c), and (d), negative values are dashed.

(e.g., Chang et al. 2000). However, the 5875-gpm contour is used in this study because it is closer to the vicinity of Taiwan than the 5880-gpm contour. The results discussed below are not sensitive to the contour that we chose. Averaged over the entire typhoon season (JJASO), the subtropical ridge tends to retreat eastward from the first to the second epoch (Fig. 5a). Because of this possible weakening of the subtropical high, the typhoon track during the second epoch tends to move a little more northward than those in the first epoch.

We further examined the subseasonal variation of the subtropical high over this region since the subtropical high over this region experiences a strong subseasonal variation (e.g., LinHo and Wang 2002). According to LinHo and Wang (2002), the entire typhoon period (JJASO) is dominated by three major natural periods in the WNP-EA region: June (the first period of summer), July–September (JAS; the second period of summer), and October (early fall). In June, the subtropical high during the second epoch tends to retreat eastward relative to the first epoch (Fig. 5b). In this period, most typhoons move westward into the South China Sea because of the strong westward extent of the subtropical high. The area where the height difference between two epochs is statistically significant is observed over the Taiwan–Philippine region. When the subtropical high retreats eastward, such as shown in Fig. 5b, the typhoon track tends to move northward. In JAS, on the other hand, the subtropical high moves northward slightly during the second epoch (Fig. 5c). This period is the peak phase of the typhoon season over the vicinity of Taiwan, which has the most typhoons passing through (Fig. 2). In this period, the subtropical high tends to move northward, so most typhoons move straight to Taiwan or turn northward to Japan and Korea. Thus, the possible northward retreat of the subtropical high (Fig. 5c) also favors the typhoon track shifting northward. In October, unlike the other two periods discussed before, the subtropical high actually becomes stronger and extends more westward (Fig. 5d), so it is not favorable for typhoons moving northward. However, the typhoon frequency in this period is lower than those in the other two periods (Chu et al. 2007). Overall, the eastward retreat of the subtropical high in JJASO, which is associated with the northward shift of typhoon track, could be a result of change of the subtropical high in summer, that is, June–September (JJAS). We note that the differences of the 500-hPa geopotential height over the western North Pacific in the peak season (JAS) are not statistically significant, possibly resulting from the small sample size of the second epoch, so the weakening of the subtropical high should be examined in the future when the second epoch becomes long enough.

We also examined the changes of other large-scale variables between two epochs. Figure 6a shows the change of low-level winds at 850 hPa. A cyclonic circulation anomaly is found between 30°N and the equator over the WNP-EA region during the second epoch, which implies a strengthening of the Asian summer monsoon trough, a favorable condition for typhoon activity. In Fig. 6b, positive and statistically significant vorticity anomalies are also found over the above-mentioned region, including Taiwan, which supports the notion of an enhanced Asian summer monsoon trough. Thus, the strengthening of the Asian summer monsoon trough is accompanied by the weakening or eastward retreat of the subtropical high shown in Fig. 5a. We note that positive low-level vorticity anomalies may also favor tropical cyclone genesis. However, it is not a dominant factor here because the number of typhoon formations is decreased over the South China Sea and the Philippine Sea. Vertical wind shear is another factor that may affect typhoon activity (Chia and Ropelewski 2002; Frank and Ritchie 2001; Gray 1979; Kurihara and Tuleya 1981). Figure 6c does show an increase of vertical wind shear in the region of 0°–15°N, 105°–150°E, which is unfavorable for typhoon formation and development, but this increase of vertical wind shear is not statistically significant. On the other hand, to the north of 15°N in the area where the low-level vorticity anomalies are positive and the cyclonic circulation anomaly dominates, the vertical wind shear has not changed appreciably, so this condition is at least not unfavorable for typhoon activity.

Another important environmental condition for tropical cyclone activity is SST. Warmer SST tends to create a favorable thermodynamic condition for tropical cyclones through the air–sea heat flux exchange (Emanuel 1999). In the North Atlantic, it is well established that SST is one of the factors impacting the number and severity of tropical cyclones (Landsea et al. 1998; Shapiro 1982; Shapiro and Goldenberg 1998). Thus, SST is examined here. In Fig. 6d, warm SST anomalies are found over the equatorial region from 120°E to 120°W. However, only the warm SST anomalies west of the date line are statistically significant. Another region with warm SST anomalies is in the North Pacific region from 30° to 50°N, which is associated with a negative phase of the Pacific decadal oscillation (Mantua et al. 1997). Both regions are away from the region with strong typhoon activity. However, SST anomalies can alter large-scale atmospheric circulation, and thus affect the typhoon track.

To understand which regions of the warm SST anomalies are responsible for creating the favorable conditions of typhoon activity over the WNP-EA region, a climate model with an intermediate complexity

(Neelin and Zeng 2000; Zeng et al. 2000) is used. In these simulations, the warm SST anomalies are prescribed separately in the equatorial region (5°S – 5°N , 130° – 175°E) and the midlatitude region (25° – 45°N , 140°E – 120°W), while a mixed layer ocean is used outside those two regions. The experiment design is similar to that used in Lau and Nath (2000). The results shown in Fig. 7 are averages of 10 ensemble runs. Given the warm SST anomalies in the equatorial region, low-level cyclonic circulation anomalies are noted over the WNP–EA region (Fig. 7a). This is a typical Rossby wave response to the equatorial warm SST anomalies (e.g., Gill 1980; Wang et al. 2003). This pattern over the WNP is qualitatively similar to that in Fig. 6a. In contrast, the warm SST anomalies over the midlatitude region have little bearing on the tropical circulation over the WNP (Fig. 7b). We note that the simulated low-level wind anomalies over the midlatitude Pacific (Fig. 7) are different than the observation shown in Fig. 6a. Thus, both the equatorial and midlatitude warm SST anomalies are not responsible for the wind anomalies over midlatitude Pacific, which may be contributed to by some complicated effects. Accordingly, the warm SST anomalies over the equatorial western and central Pacific are postulated as a possible cause for inducing the favorable conditions for the northward shift of the typhoon track. We then examine the temporal variation of the SST over the equatorial region.

Figure 8 shows the time series of monthly SST anomalies, with the annual cycle removed, along the equatorial western and central Pacific (5°S – 5°N , 130° – 175°E) from 1982 to July 2007. The SST anomalies exhibit an interannual variation, which is roughly related to the three strongest El Niño events of the twentieth century: 1982/83, 1991/92, and 1997/98, a sharp reduction of the SST anomalies from the growing year (the year before the El Niño peak phase, such as 1997) to the decaying year (the year after the El Niño peak phase, such as 1998). We used the regression model discussed in Chu (2002) to analyze the variation of the monthly SST anomalies. A statistically significant shift occurs in August 2000 (Fig. 8). Specifically, before August 2000, the average of the SST anomalies is about -0.1°C , but it increases to 0.3°C after August 2000. Although this difference seems to be small, it is considerable when viewed in the context of multiyear seasonal means at the equator. In the interannual time scale, the typhoon number over the vicinity of Taiwan is also strongly associated with the SST anomalies over the equatorial western and central Pacific (C.-T. Lee 2008, personal communication). We also examined the six typhoons that passed through the vicinity of Taiwan in 2000 and found that five out of six typhoons occurred in or after August

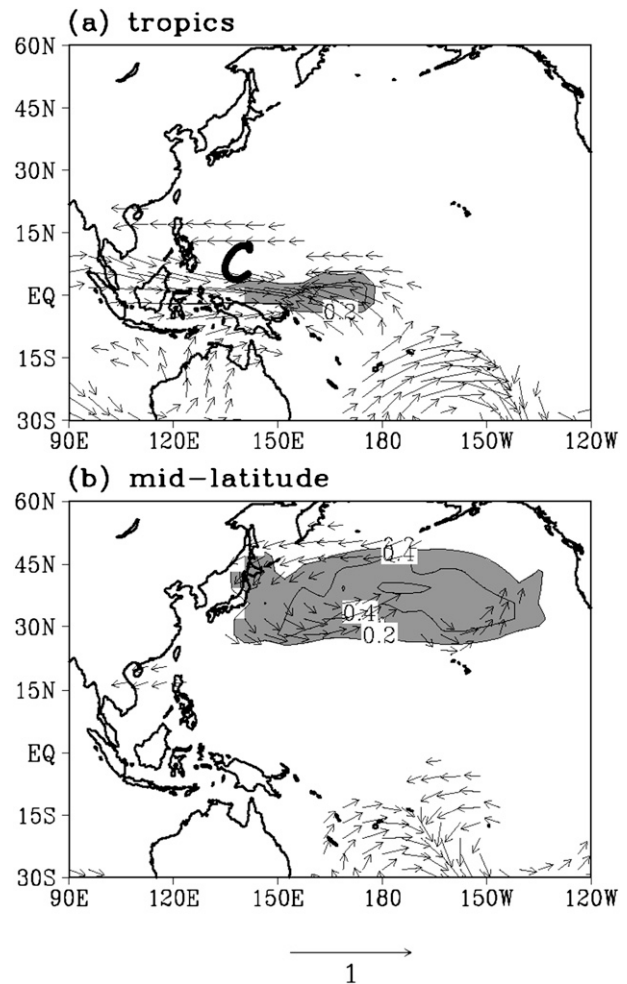


FIG. 7. SST anomalies (contour) and 850-hPa wind anomalies from the model simulations with the prescribed SST anomalies over (a) the equatorial region (5°S – 5°N , 130° – 175°E) and (b) midlatitudes (25° – 45°N , 140°E – 120°W).

2000. After further examining the SST anomalies in 2007, we found that warm SST anomalies still exist over the equatorial western and central Pacific (Fig. 8), which is consistent with the above-normal number of typhoons (five) that we found so far in 2007. Thus, combining results from observations, especially in Figs. 3 and 8, and model simulations, the warm SST anomalies over the equatorial western to central Pacific appear to be main factors that induced the abrupt change of the northward shift of the typhoon track over the WNP–EA region.

5. Discussion and conclusions

Long-term climate variability of typhoon activity over the western North Pacific–East Asian (WNP–EA) sector has been analyzed here. Because Taiwan is located at a unique location along the typhoon path, the number

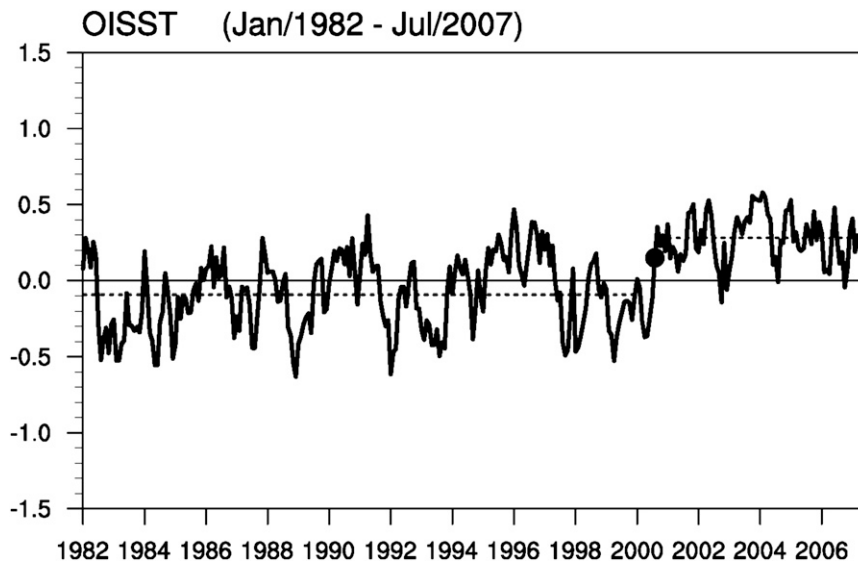


FIG. 8. Variation of monthly SST anomalies averaged over the area of 5°S – 5°N , 130° – 175°E from January 1982 to July 2007. The short dashed lines are the means averaged over 1982–99 (-0.1°C) and 2001–06 (0.3°C), respectively.

of typhoons that pass through the vicinity of Taiwan is used to study the movement of the typhoon track over this region. Our analysis suggests an abrupt change in typhoon numbers in 2000, which is consistent with the northward shift of the typhoon track over the WNP–EA region and the abrupt increase of typhoon frequency over the Taiwan–East China Sea region. This northward shift of the typhoon track is mainly associated with warm SST anomalies over the equatorial western and central Pacific, which exhibited an abrupt change in August 2000, concurrent with the change of the typhoon track. Both observations and model simulations show that the equatorial warm SST anomalies tend to induce an eastward and northward retreat of the subtropical high, an enhanced low-level vorticity, and a monsoon trough, which all favor the northward shift of the typhoon track.

Under global warming, El Niño-like warm SST anomalies are often found over the equatorial Pacific region (Meehl and Washington 1996; Meehl et al. 2007; Teng et al. 2006). In this study, we also found that the mean state of the equatorial Pacific SST transitioned from a cold to a warm phase in 2000. The question that arises is as follows: Do the equatorial SST anomalies that are associated with the abrupt northward shift of the typhoon track over the WNP–EA region result from global warming? This is an interesting question that should be answered in the future.

Acknowledgments. This work was supported by the National Science Council Grants 96-2628-M-001-019 and 97-2111-M-034-001-MY2. Comments from the

anonymous reviewers were helpful for improving the quality of this paper.

REFERENCES

- Betts, A. K., and M. J. Miller, 1993: The Betts–Miller scheme. *The Representation of Cumulus Convection in Numerical Models of the Atmosphere*, Meteor. Monogr., No. 46, Amer. Meteor. Soc., 107–121.
- Camargo, S. J., A. W. Robertson, S. J. Gaffney, P. Smyth, and M. Ghil, 2007: Cluster analysis of typhoon tracks. Part I: General properties. *J. Climate*, **20**, 3635–3653.
- Carlin, B. P., and T. A. Louis, 2000: *Bayes and Empirical Bayes Methods for Data Analysis*. Chapman & Hall/CRC, 419 pp.
- Chan, J. C. L., 1985: Tropical cyclone activity in the northwest Pacific in relation to the El Niño/Southern Oscillation phenomenon. *Mon. Wea. Rev.*, **113**, 599–606.
- , 2000: Tropical cyclone activity over the western North Pacific associated with El Niño and La Niña events. *J. Climate*, **13**, 2960–2972.
- , and K. S. Liu, 2004: Global warming and western North Pacific typhoon activity from an observational perspective. *J. Climate*, **17**, 4590–4602.
- Chang, C.-P., Y. Zhang, and T. Li, 2000: Interannual and interdecadal variations of the East Asian summer monsoon and tropical Pacific SSTs. Part I: Roles of the subtropical ridge. *J. Climate*, **13**, 4310–4325.
- Chia, H.-H., and C. F. Ropelewski, 2002: The interannual variability in the genesis location of tropical cyclones in the northwest Pacific. *J. Climate*, **15**, 2934–2944.
- Chu, P.-S., 2002: Large-scale circulation features associated with decadal variations of tropical cyclone activity over the central North Pacific. *J. Climate*, **15**, 2678–2689.
- , 2004: ENSO and tropical cyclone activity. *Hurricanes and Typhoons: Past, Present, and Potential*, R. J. Murnane and K. B. Liu, Eds., Columbia University Press, 297–332.

- , and X. Zhao, 2004: Bayesian change-point analysis of tropical cyclone activity: The central North Pacific case. *J. Climate*, **17**, 4893–4901.
- , —, C.-T. Lee, and M.-M. Lu, 2007: Climate prediction of tropical cyclone activity in the vicinity of Taiwan using the multivariate least absolute deviation regression method. *Terr. Atmos. Oceanic Sci.*, **18**, 805–825.
- Doney, S. C., W. G. Large, and F. O. Bryan, 1998: Surface ocean fluxes and water-mass transformation rates in the coupled NCAR climate system model. *J. Climate*, **11**, 1420–1441.
- Elsner, J. B., and T. Jagger, 2004: A hierarchical Bayesian approach to seasonal hurricane modeling. *J. Climate*, **17**, 2813–2827.
- , —, and J.-F. Niu, 2000: Changes in the rates of North Atlantic major hurricane activity during the 20th century. *Geophys. Res. Lett.*, **27**, 1743–1746.
- Emanuel, K. A., 1999: Thermodynamic control of hurricane intensity. *Nature*, **401**, 665–669.
- , 2005: Increasing destructiveness of tropical cyclones over the past 30 years. *Nature*, **436**, 686–688.
- Epstein, E. S., 1985: *Statistical Inference and Prediction in Climatology: A Bayesian Approach*. Meteor. Monogr., No. 42, Amer. Meteor. Soc., 199 pp.
- Frank, W. M., and E. A. Ritchie, 2001: Effects of vertical wind shear on the intensity and structure of numerically simulated hurricanes. *Mon. Wea. Rev.*, **129**, 2249–2269.
- Gill, A. E., 1980: Some simple solutions for heat induced tropical circulation. *Quart. J. Roy. Meteor. Soc.*, **106**, 447–462.
- Gray, W. M., 1979: Hurricanes: Their formation, structure and likely role in the general circulation. *Meteorology over the Tropical Oceans*. D. B. Shaw, Ed., Royal Meteorological Society, 155–218.
- Hansen, J., I. Fung, A. Lacis, D. Rind, S. Lenedeff, R. Ruedy, and G. Russell, 1988: Global climate changes as forecast by Goddard Institute for Space Studies three-dimensional model. *J. Geophys. Res.*, **93D**, 9341–9364.
- , M. Sato, and R. Ruedy, 1997: Radiative forcing and climate response. *J. Geophys. Res.*, **102**, 6831–6864.
- Ho, C.-H., J.-J. Baik, J.-H. Kim, D.-Y. Gong, and C. H. Sui, 2004: Interdecadal changes in summertime typhoon tracks. *J. Climate*, **17**, 1767–1776.
- , J.-H. Kim, J.-H. Jeong, H.-S. Kim, and D. Chen, 2006: Variation of tropical cyclone activity in the south Indian Ocean: El Niño–Southern Oscillation and Madden-Julian Oscillation effects. *J. Geophys. Res.*, **111**, D22101, doi:10.1029/2006JD007289.
- Hoyos, C. D., P. A. Agudelo, P. J. Webster, and J. A. Curry, 2006: Deconvolution of the factors contributing to the increasing global hurricane intensity. *Science*, **312**, 94–97.
- Kanamitsu, M., W. Ebisuzaki, J. Woollen, S.-K. Yang, J. J. Hnilo, M. Fiorino, and G. L. Potter, 2002: NCEP-DOE AMIP-II Reanalysis (R-2). *Bull. Amer. Meteor. Soc.*, **83**, 1631–1643.
- Keith, D. W., 1995: Meridional energy transport: Uncertainty in zonal means. *Tellus*, **47A**, 30–44.
- Kim, J.-H., C.-H. Ho, and C.-H. Sui, 2005: Circulation features associated with the record-breaking typhoon landfall on Japan in 2004. *Geophys. Res. Lett.*, **32**, L1472, doi:10.1029/2005GL022494.
- Klotzbach, P. J., 2006: Trends in global tropical cyclone activity over the past twenty years (1986–2005). *Geophys. Res. Lett.*, **33**, L10805, doi:10.1029/2006GL025881.
- Kurihara, Y., and R. E. Tuleya, 1981: A numerical-simulation study on the genesis of a tropical storm. *Mon. Wea. Rev.*, **109**, 1629–1653.
- Landsea, C. W., G. D. Bell, W. M. Gray, and S. B. Goldenberg, 1998: The extremely active 1995 Atlantic hurricane season: Environment condition and verification of seasonal forecasts. *Mon. Wea. Rev.*, **126**, 1174–1193.
- , B. A. Harper, K. Hoarau, and J. A. Knaff, 2006: Can we detect trends in extreme tropical cyclones? *Science*, **313**, 452–454.
- Lau, N.-C., and M. J. Nath, 2000: Impact of ENSO on the variability of the Asian-Australian monsoons as simulated in GCM experiments. *J. Climate*, **13**, 4287–4309.
- Levinson, D. H., and Coauthors, 2005: State of the climate in 2004. *Bull. Amer. Meteor. Soc.*, **86**, S1–S86.
- LinHo, and B. Wang, 2002: The time–space structure of the Asian–Pacific summer monsoon: A fast annual cycle view. *J. Climate*, **15**, 2001–2019.
- Mantua, N. J., S. R. Hare, Y. Zhang, J. M. Wallace, and R. C. Francis, 1997: A Pacific interdecadal climate oscillation with impacts on salmon production. *Bull. Amer. Meteor. Soc.*, **78**, 1069–1079.
- Matsuura, T., M. Yumoto, and S. Iizuka, 2003: A mechanism of interdecadal variability of tropical cyclone activity over the western North Pacific. *Climate Dyn.*, **21**, 105–117.
- Meehl, G. A., and W. M. Washington, 1996: El Niño-like climate change in a model with increased atmospheric CO₂ concentrations. *Nature*, **382**, 56–60.
- , and Coauthors, 2007: Global climate projection. *Climate Change 2007: The Physical Science Basis*, S. Solomon et al. Eds., Cambridge University Press, 747–845.
- Miller, J. R., G. L. Russell, and L.-C. Tsang, 1983: Annual oceanic heat transports computed from an atmospheric model. *Dyn. Atmos. Oceans*, **7**, 95–109.
- Neelin, J. D., and J.-Y. Yu, 1994: Modes of tropical variability under convective adjustment and the Madden–Julian oscillation. Part I: Analytical theory. *J. Atmos. Sci.*, **51**, 1876–1894.
- , and N. Zeng, 2000: A quasi-equilibrium tropical circulation model—Formulation. *J. Atmos. Sci.*, **57**, 1741–1766.
- Ren, F., G. Wu, W. Dong, X. Wang, Y. Wang, W. Ai, and W. Li, 2006: Changes in tropical cyclone precipitation over China. *Geophys. Res. Lett.*, **33**, L20702, doi:10.1029/2006GL027951.
- Reynolds, R. W., N. A. Rayner, T. M. Smith, D. C. Stokes, and W. Wang, 2002: An improved in situ and satellite SST analysis for climate. *J. Climate*, **15**, 1609–1625.
- Russell, G. L., J. R. Miller, and L.-C. Tsang, 1985: Seasonal oceanic heat transports computed from an atmospheric model. *Dyn. Atmos. Oceans*, **9**, 253–271.
- Shapiro, L. J., 1982: Hurricane climate fluctuations. Part II: Relation to large-scale circulation. *Mon. Wea. Rev.*, **110**, 1014–1040.
- , and S. B. Goldenberg, 1998: Atlantic sea surface temperature and tropical cyclone formation. *J. Climate*, **11**, 578–590.
- Stowasser, M., Y. Wang, and K. Hamilton, 2007: Tropical cyclone changes in the western North Pacific in a global warming scenario. *J. Climate*, **20**, 2373–2396.
- Teng, H., L. E. Buja, and G. A. Meehl, 2006: Twenty-first-century climate change commitment from a multi-model ensemble. *Geophys. Res. Lett.*, **33**, L07706, doi:10.1029/2005GL024766.
- Wang, B., and J. C. L. Chan, 2002: How ENSO regulates tropical storm activity over the western North Pacific. *J. Climate*, **15**, 1643–1658.
- , R. Wu, and T. Li, 2003: Atmosphere–warm ocean interaction and its impacts on Asian–Australian monsoon variation. *J. Climate*, **16**, 1195–1211.

- Webster, P. J., G. J. Holland, J. A. Curry, and H. R. Chang, 2005: Changes in tropical cyclone number, duration and intensity in a warm environment. *Science*, **309**, 1844–1846.
- Wu, L., and B. Wang, 2004: Assessing impacts of global warming on tropical cyclone tracks. *J. Climate*, **17**, 1686–1698.
- , —, and S. Geng, 2005: Growing typhoon influence on east Asia. *Geophys. Res. Lett.*, **32**, L18703, doi:10.1029/2005GL022937.
- Yu, J.-Y., and J. D. Neelin, 1994: Modes of tropical variability under convective adjustment and the Madden–Julian oscillation. Part II: Numerical results. *J. Atmos. Sci.*, **51**, 1895–1914.
- Zeng, N., J. D. Neelin, and C. Chou, 2000: The first quasi-equilibrium tropical circulation model-implementation and simulation. *J. Atmos. Sci.*, **57**, 1767–1796.
- Zhao, Z., and P.-S. Chu, 2006: Bayesian multiple change point analysis of hurricane activity in the eastern North Pacific: A Markov chain Monte Carlo approach. *J. Climate*, **19**, 564–578.